PHYSICAL AND MECHANICAL PROPERTIES OF

COMMON ASH (*FRAXINUS EXCELSIOR* L.)

Peter Niemz, Sebastian Clauss, Franco Michel
Institute for Building Materials, Eth Zurich
Zűrich, Switzerland

Daniel Hänsch, Andreas Hänsel
University of Cooperative Education
Dresden, Germany

ABSTRACT

Nowadays hardwood is increasingly used in timber construction, partly as a substitute for softwood members and partly in combination with softwood. In principle, hardwood shows orthotropic behavior similar to softwood. However, the magnitudes and the ratios of the mechanical parameters between the three anatomical directions differ and depend strongly on the individual microstructure of the species. The aim of our study was to characterize the orthotropic mechanical behavior of common ash (*Fraxinus excelsior* L.) under varying equilibrium wood moisture conditions. As a result, we determined a dataset of selected moisture dependent elastic and strength parameters for different load types and orientations. Furthermore, important physical properties of ash, such as differential swelling ratio, water absorption coefficient, water vapor resistance and thermal conductivity, were obtained within this study.

KEYWORDS: Ash wood, mechanical properties, physical properties, moisture content, orthotropy.

INTRODUCTION

In the forests of central Europe, a semi-natural forestry tendency is observable. Thus, over the long term, a higher percentage of hardwood will develop within tree populations. Yet, a decrease of 40 % in hardwood production and a reduction in use of about 50 % was recorded for hardwood in the last decade, for example, in Switzerland (Krackler et al. 2010, Bonoli et al. (2005), Krackler et al. 2011). Further, substitution materials such as synthetic materials, metals, and concrete, as well as other wood products has by reduced the demand for hardwood products. As a consequence, about 60 % of the harvest is directly utilized for energy purposes without

contributing to the value chain (Krackler 2010). Thus a more holistic use of the hardwood natural resource is worth consideration. Potentially, hardwood would be increasingly used if more detailed species specific data in relation to construction relevant data were available.

In spite of the various publications in this area, the determination of parameters needed in material models is still a challenging question, since comprehensive datasets for individual wood species are rare. As is well known in the case of wood, the mechanical properties differ significantly within the three anatomical directions: Longitudinal, radial and tangential. Additionally, they deviate between individual species, from tree to tree and within the tree.

Selected property parameters of hardwood have been published by Kollmann (1941, 1951), Bodig and Jayne (1993), Szalai (1994), Požgaj et al. (1997), Sell (1997), Wagenführ (2007), and Horvath et al. 2008 amongst others. However, complete datasets with moisture dependent parameters in the three main wood directions, usable for finite element modeling, rarely exist. These are necessary for static calculations and wood construction modeling, as well as for cupping or warping deformation calculations of multi-layered boards (Blumer et al. 2009, Gereke et al. 2009), parquet, furniture and musical instruments. The majority of investigations are carried out parallel to the grain under tension, compression or bending. Parameters of the other main directions, transverse to the grain, which are required for finite element calculations, as well as the influences of fiber and growth ring angle, are limited for hardwood or not available. Equally, the influences of the load type (tension, compression, bending) and moisture content on the elastic constants and the Poisson's ratio have been scarcely investigated.

MATERIAL AND METHODS

Material

The investigated wood species (*Fraxinus excelsior* L.) originates from Eastern Switzerland with a mean normal density ρ_{12} of 0.640 g·cm^{-3} (at an equilibrium moisture content (EMC) of about 12 %). The clear specimens were cut from the same trunk (a single stem). Intrinsic knots and defects were excluded.

To obtain a comprehensive dataset of the mechanical and physical properties of ash, the following characteristic values were determined:

- Differential swelling ratio
- Water absorption coefficient (liquid water)
- Water vapor resistance (dry and wet cup)
- Thermal conductivity (in 20°C/65 % RH)

The mechanical properties were tested at 20°C at the relative humidities (RH) 35, 65, 85 and 95 % (depending on the test method used). The EMC of the wood samples was determined for each climate. Tests were performed for the different anatomical directions: Radial (R), tangential (T) and longitudinal (L), and respectively, for the planes arising from these. The following mechanical properties were measured:

- MOE: Bending, tension, compression, eigenfrequency, ultrasound
- Shear modulus: Ultrasound
- Strength: Tension, compression, bending

- Poisson's ratio: Compression
- Fracture toughness

Determination of the physical properties

Differential swelling

The differential swelling ratio was determined in the L-, R- and T-directions in four climatic steps between 35 and 95 % RH according to DIN 52184 (1979). A total of 30 specimens, sized 20 (R) × 20 (T) × 100 (L) mm, were prepared for the L-direction. 30 specimens sized 50 (R) × 50 (T) × 10 (L) mm, were used for the R and T-directions.

Water vapor resistance

The water vapor resistance factor in the R- and T-directions was determined according to DIN EN ISO 12572 (2001) at dry (20°C/65 % RH) and wet (20°C/100 % RH) conditions. For each climate condition and anatomic direction, six specimens with a diameter of 140 mm and a thickness of 20 mm were tested.

Water absorption

The water absorption coefficient $Aw[kg \cdot (m^{-2} \cdot s^{0.5})]$ was determined in the L-, R- and T-directions of cubes with side lengths of 50 mm according to DIN EN ISO 15148 (2003). Four sides of the cube were varnished with a synthetic resin lacquer to ensure that water absorption occurred only in one direction. The specimens were conditioned in normal climate (20°/65 % RH) prior to the test. Then the specimens were put on a grid and placed 5±2 mm deep into a water bath where the mass gain per face area Δm (kg·m^{-2}) was weighed after 5 and 20 minutes and at 1, 2, 4, 8, 11 and 24 hours. 20 cubes were tested for each anatomical direction.

Thermal conductivity

According to ISO 8302 (1991) the thermal conductivity was tested perpendicular to the grain on three solid-wood boards (500 × 500 × 20 mm) with the guarded hot plate apparatus λ-Meter EP500 (Lambda-Messtechnik GmbH, Dresden). The specimens were conditioned in normal climate (20°C/65 % RH). After conditioning, thermal conductivity was measured at three temperatures (10, 20 and 30°C). Each measurement was performed with a temperature difference of 10 K between the hot and cold plates and a surface pressure of 2500 N. m^{-2}.

Determination of the mechanical properties

Dynamic testing methods

Sound velocity and eigenfrequency were determined on the same specimens (20 (R) × 20 (T) × 400 (L) mm) used for the bending test. Dynamic testing was performed with an ultrasound device (BP-V, frequency 50 kHz, Steinkamp, Bremen). The dynamic stiffness was calculated from the sound velocity c and the density ρ with the basic relation shown in Eq. 1.

$$E = \rho \cdot c^2 \tag{1}$$

Since this formula is a rough approximation, with exaggerated values in comparison to the results of the static testing method, a correction (Eq. 2) of the data based on the Poisson's ratios in compression determined especially for high ultrasound frequencies was used according to Bucur (2006).

$$E_1 = C_{11}k_1 = \rho V_{11}^2 \frac{1 - v_{12}v_{21} - v_{23}v_{32} - v_{13}v_{31} - 2v_{21}v_{32}v_{13}}{1 - v_{23}v_{32}}$$

$$E_2 = C_{22}k_2 = \rho V_{22}^2 \frac{1 - v_{12}v_{21} - v_{23}v_{32} - v_{13}v_{31} - 2v_{21}v_{32}v_{13}}{1 - v_{31}v_{13}} \qquad (2)$$

$$E_3 = C_{33}k_3 = \rho V_{33}^2 \frac{1 - v_{12}v_{21} - v_{23}v_{32} - v_{13}v_{31} - 2v_{21}v_{32}v_{13}}{1 - v_{12}v_{21}}$$

The MOE based on the eigenfrequency (E_{ef}) of the first flexural mode was determined according to the method by Görlacher (1984), using an eigenfrequency tester (Grindosonic MK 5, Industrial, Lemmens N. V., Belgium).

Additionally, the MOE in the 3 main directions (Eqs. 1 and 2) and the shear modulus (G) (Eq. 3) were determined by ultrasound means. 20 cuboid specimens with a side length of 10 mm were tested at a temperature of 20°C and different RH of 45, 65 and 85 %. The experiments were performed with an EPOCH XT device (Olympus NDT Inc., USA), using an Olympus A133S transducer (2.27 MHz) for longitudinal waves (determination of MOE) and a Staveley S-0104 transducer (1 MHz) for transverse waves (determination of G), with the coupling agent Ultragel II (Sonotech, USA).

$$G_{ij} = c_{ij}^2 \cdot \rho \qquad (3)$$

The shear modulus is related to the square of the sound velocity c and the density ρ of the specimen (Eq. 3). Thereby, the directions of wave propagation (first index) and the direction of wave oscillation (second index) are exchangeable for an orthotropic material. The values of G_{ij} and G_{ji} were averaged.

Bending test

According to DIN 52186 (1978), the bending strength and the static MOE (parallel to the fiber direction) were determined on 20 specimens sized 20 (R) × 20 (T) × 400 mm (L) using a universal testing machine (Zwick GmbH & Co. KG, Ulm).

Tension test

Tensile strength and tensile modulus (MOE) were determined parallel and perpendicular to the grain. The strength test was performed in accordance to the standard DIN 52187 (1979) in the longitudinal direction. To determine the radial and tangential properties, dog-bone shaped specimens of 95 mm length with varying cross sectional areas (max. 28 × 28, min. 14 × 14 mm) were used. 10 specimens were tested for each anatomical direction and climate. In the longitudinal direction, the experiments were conducted with a Zwick Z100, whereas the radial and tangential tests were performed using a Zwick Z010. For determination of the Poisson's ratios the longitudinal and transverse deformations were determined with a video image correlation system (Vic 2D, LIMESS Messtechnik& Software GmbH, Krefeld). This method is described in detail by Keunecke et al. (2007) and Hering (2011).

Compression test

Compression strength parallel to the grain was determined according to DIN 52185 (1976) and perpendicular to the grain according to DIN 52192 (1979). However, a reduced specimen size (15 × 15 × 45 mm) was used. 20 specimens were tested in every direction and climate. Equivalent to the tensile tests, the Poisson's ratios were determined by means of a video image correlation system.

Fracture toughness test

The fracture toughness (K_{IC}) in the RL, TL, RT and TR planes (first index: Direction normal to the crack plane, second index: Direction of crack propagation) was determined according to DIN EN ISO 12737 (2011). A total of 10 compact specimens per direction and climate were used using a Zwick Z100 testing machine in combination with a video-extensometer.

RESULTS AND DISCUSSION

Physical properties

The differential swelling of the tested samples amounted to 0.01 %/% in the L direction (Tab. 1). The R and T values amounted to 0.19 and 0.39 %/%, respectively. Similar values are presented in the literature by Grosser und Teetz (1985).

The water vapor resistances perpendicular to the grain, determined with dry and wet cup tests, are shown in Tab 1. For both, wet and dry cup tests, the water vapor resistances in the R direction is larger than in the T direction. This difference is affected by the radially oriented wood rays. Values obtained by dry cup tests are twice as high as values obtained by wet cup tests.

The capillary water absorption coefficients (A_w) of ash for the three anatomical directions are summarized in Tab. 1. The water absorption coefficient parallel to the fibers is eight times higher (0.0294 kg·m^{-2}s$^{0.5}$) than when measured perpendicular to the fibers. Additionally, the capillary water absorption in the radial direction (0.0042 kg·m^{-2}s$^{0.5}$) is higher than in the tangential direction (0.0032 kg·m^{-2}s$^{0.5}$). The measured values for ash are in the range of other hardwoods like beech and oak (Sonderegger et al. 2012).

For a comparison: For specimens with a raw density of 0.688 g·cm^{-3}, Krackler et al. (2010) determined values of 0.0098 kg·m^{-2}s$^{0.5}$ in the longitudinal, 0.0030 kg·m^{-2}s$^{0.5}$ in the radial and 0.0033 kg·m^{-2}s$^{0.5}$ in the tangential direction. Sonderegger et al. (2012) determined values of about 0.0121 kg·m^{-2}s$^{0.5}$ in the longitudinal, 0.0026 kg.m^{-2}s$^{0.5}$ in the radial and 0.0034 kg·m^{-2}s$^{0.5}$ in the tangential direction (density 0.64-0.77 g·cm^{-3}). The values measured perpendicular to the grain are in accordance with the here presented measurements.

The measured thermal conductivity of 0.14 W/mK is within the range of other hardwoods with comparable raw density, e.g. oak and beech, while Grosser and Teetz (1985) found a higher thermal conductivity of 0.17 W/mK for ash.

Tab. 1: Physical properties of ash; q = swelling ratio; μ_{dry}, μ_{wet} = water vapor resistance factors at dry and wet conditions; A_w = water absorption coefficient; λ_{10} = thermal conductivity at 10°C; (ω) = coefficient of variation in %; thermal conductivity and water uptake tested after conditioning at 20°C/65 % RH.

Parameter	Mean		Orientation	n
q (%/%)	0.01	(23.5)	L	30
	0.19	(4.8)	R	30
	0.39	(2.0)	T	30
μ_{dry} (-)	157.5	(6.5)	R	6
	116.2	(4.9)	T	6
μ_{wet} (-)	30.8	(6.5)	R	6
	22.5	(5.7)	T	6
A_w (kg·(m^{-2}·s$^{0.5}$)	0.0294	(3.5)	L	20
	0.0042	(19.5)	R	20
	0.0032	(15.1)	T	20
λ_{10} (W/(m·K))	0.136	(-)	R/T	3

Mechanical properties

Bending and dynamic MOE

The moisture dependent MOE_s determined by static bending measurements and dynamic tests (sound propagation and eigenfrequency) in the longitudinal direction, are summarized in Tab. 2 and Fig. 1a. The highest MOE (E_{BP5}) as obtained by ultrasonic measuring with the BP5-System. Taking shear effects (Eq. 3, Bucur 2006) into consideration, the MOE (E_{BP5}) values are 15 % higher than the static MOE ($E_{bending}$). This is triggered by the samples' ratio of length to thickness and the frequency.

Tab. 2: Moisture dependent values (longitudinal direction) obtained through static bending and dynamic tests (n=20); ρ_{12}=0.58–0.62 g·cm^{-3};(ω) = coefficient of variation in %.

ω (%)		E_{eF} (MPa)		E_{BP5} (MPa)		$E_{bending}$(MPa)		$\sigma_{bending}$(MPa)	
8.2	(1.6)	11747	(11)	14522	(12)	12623	(12)	116	(8)
13.4	(5.0)	11527	(9)	13945	(10)	12371	(10)	95	(5)
17.5	(2.6)	11437	(11)	14006	(9)	12011	(12)	81	(15)
18.8	(4.6)	11104	(13)	13776	(12)	11622	(14)	78	(9)

The MOE based on eigenfrequency (E_{eF}) measurements are similar to the static values ($E_{bending}$). As expected, the MOE decreases with increasing EMC (Fig. 1a).

The MOE in the R and T directions obtained with the EPOCH XT method (Tab. 3) reveal a dependency on the EMC as well. These values are much higher in relation to static tests. After correcting the Poisson's effect, the results (Tab. 3) were better correlated in relation to static MOE tests (Tabs. 5 and 6).

Tab. 3: Results of MOE for dynamic tests (with EPOCH XT) in the L, R, and T directions on cubes (n=20) uncorrected and corrected (*, with the method described by (Bucur 2006) for different EMC; ρ_{12} = 0.59–0.61 g·cm^{-3}; (ω) = coefficient of variation in %.

ω (%)		E_L (MPa)		E_R (MPa)		E_T (MPa)		E_{L^*} (MPa)	E_{R^*} (MPa)	E_{T^*} (MPa)
7.9	(5.0)	19713	(5)	3286	(6)	1990	(9)	14305	2460	1493
10.1	(1.0)	18868	(6)	3155	(5)	1904	(10)	10'848	2168	1337
14.1	(1.0)	18006	(6)	2858	(4)	1623	(6)	8591	1956	1130
15.9	(1.0)	18104	(5)	2691	(6)	1463	(8)	8'32	1797	1009

Shear modulus

As expected, the dynamically determined shear modulies (Tab. 4) and the MOEs show a significant correlation with the EMC. The highest G was found in the LR plane, followed by the values in the LT and RT planes (Fig. 1c). The dynamically obtained values (G_{LR}=1410, G_{LT}=620, G_{RT}=511 MPa) of Keunecke et al. (2008) are in good agreement with the results obtained. Further, our results are in agreement with the measurements of Bucur (2006) (G_{LR}=1340, G_{LT}=890, G_{RT}=270 MPa). However, again, the significantly higher density (ρ=0.67 g·cm^{-3} (Bucur 2006) has to be taken into account.

Tab. 4: Results of shear modulus for dynamic tests with EPOCH XT (n=20); ρ_{12}=0.59–0.61 g·cm^{-3}; (ω) = coefficient of variation in %.

ω (%)		G_{LR} (MPa)		G_{LT} (MPa)		G_{RT} (MPa)	
8.2	(1.6)	1283	(2.8)	1050	(16.9)	357	(8.5)
13.4	(5.0)	1177	(6.5)	812	(6.9)	382	(17.9)
17.5	(2.6)	1031	(10.4)	806	(3.9)	263	(6.5)
18.8	(4.6)	964	(5.5)	780	(6.6)	246	(9.9)

Tensile and compression MOE

The elastic properties at standard climatic conditions correspond to values found in the literature (see Bodig and Jayne (1993), Požgaj et al. (1997)). The MOE decreased with increasing EMC (Figs. 1a, b). We also found similar MOE values for tension and compression tests in the longitudinal and tangential directions. A comparison of values from the literature always reveals a high variation in the results. This variance is impressively demonstrated in the monograph about ash by Kollmann (1941). The values of MOE for ash with a density of 0.670 g·cm^{-3} and an EMC of 11 %, shown in Ross (2010), reveal values of E_L=13700, E_R=1510 and E_T=800 MPa.
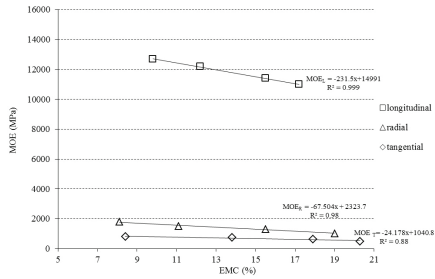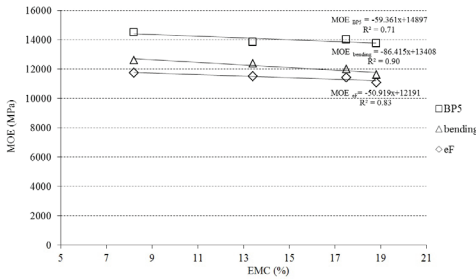

Fig. 1: a) MOE in the fiber direction dependent on test method.

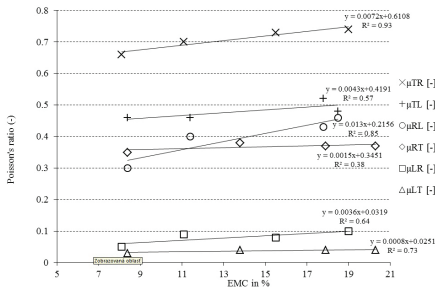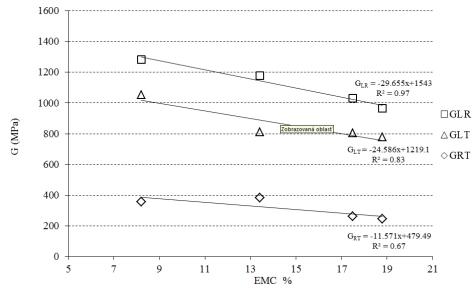*Fig. 1: b) MOE in the main directions in tension.*

Fig. 1: c) G module tested with ultrasound.

Fig. 1: d) Poisson's ratio tested in compression.

Poisson's ratios

The Poisson's ratios for the compression test in the individual planes are illustrated in Tab. 5. The obtained values are in agreement with results obtained by Niemz (1993) and Požgaj et al. (1997).

Tab. 5: MOE and strength properties under tension load (n=10); ρ_{12} = 0.59–0.62 g·cm^{-3}; (ω) =coefficient of variation in %.

Orientation	ω (%)		E$_t$ (MPa)		σ$_t$ (MPa)	
	9.8	(3.1)	12700	(8.0)	134	(11)
L	12.2	(3.7)	12200	(13.8)	130	(13)
	15.5	(1.9)	11400	(13.8)	129	(16)
	17.2	(1.3)	11000	(12.3)	125	(16)
	8.1	(1.3)	1810	(8.0)	15.8	(5.0)
R	11.1	(1.5)	1510	(16.8)	12.5	(8.0)
	15.5	(0.6)	1320	(6.0)	12.3	(5.7)
	19.0	(1.0)	1030	(9.1)	11.2	(6.8)
	8.4	(1.0)	804	(5.9)	9.2	(3.6)
T	13.8	(0.7)	759	(7.7)	8.3	(5.7)
	17.9	(1.4)	635	(11.6)	7.6	(2.9)
	20.3	(1.1)	505	(9.8)	6.6	(3.9)

The Poisson's ratio increased with the EMC (Fig. 1d). No clear tendency in the literature can be found for the EMC and Poisson's ratio relation.In contrast to results by Sonderegger et al. (2012) for sycamore maple, no significant tendency was found for EMC. This was also stated for European beech by Ozyhar et al. (2012b). In contrast, Hering et al. (2012) observed a decrease of Poisson's ratio with increasing EMC for beech in all directions.

Tab. 6: Elastic and strength properties under compression load, perpendicular to the grain for 0.2 % plastic deformation (n = 20); ρ_{12} = 0.55–0.62 g·cm^{-3}; (ω) = coefficient of variation in %.

*	ω (%)		E$_c$ (MPa)		σ$_c$ (MPa)		μ$_{RL}$ (-)		μ$_{TL}$ (-)		μ$_{LR}$ (-)		μ$_{TR}$ (-)		μ$_{LT}$ (-)		μ$_{RT}$ (-)	
	8.4	(1.0)	12110	(13)	55	(11)	0.3	(29.7)	0.46	(17.1)								
L	11.4	(1.0)	9221	(10)	43	(3)	0.4	(19.4)	0.46	(19.4)								
	17.8	(1.3)	9908	(22)	37	(4)	0.43	(33.1)	0.52	(24.6)								
	18.5	(0.7)	8922	(12)	32	(5)	0.46	(10.9)	0.48	(18.4)								
	8.1	(1.3)	1695	(21)	12.4	(3.5)					0.05	(129)	0.66	(8.7)				
R	11.1	(1.5)	1368	(7)	10.5	(4.4)					0.09	(18.5)	0.7	(4.9)				
	15.5	(0.6)	1139	(7)	8.3	(1.0)					0.08	(32.4)	0.73	(3.2)				
	19.0	(1.0)	1024	(7)	7.7	(5.0)					0.10	(26.2)	0.74	(4.1)				
	8.4	(1.0)	965	(12)	13.8	(1.3)									0.03	(48.1)	0.35	(4.5)
T	13.8	(0.7)	643	(6)	10.0	(3.6)									0.04	(42.1)	0.38	(10.0)
	17.9	(1.4)	530	(4)	8.0	(1.6)									0.04	(23.4)	0.37	(3.3)
	20.3	(1.1)	434	(7)	7.0	(2.3)									0.04	(36.8)	0.37	(3.1)

* Orientation

Strength properties

Tensile, compression and bending strength

Tabs. 5 and 6 summarize the strength measurements obtained in the compression and tension tests. The EMC has a significant effect on this parameter. Within the investigated range of about 8 to 20 %, the strength decreases linearly with increasing EMC (Fig. 2). Similar trends have already been documented in the literature. An increase in strength in the range between oven dry state and 10 % EMC was reported in several studies (Ross 2010, Szalai et al. 2004). This range was not investigated in the current study since the practical application is minor. The internal stresses led to an increase of the ultimate strength and a decrease of the plastic

deformability (Kollmann 1951). This implies that the notch stresses cannot be reduced. Although the MOE of ash is similar to that of conifers, like spruce. The longitudinal strength under tension (σ_t=130 MPa) is significantly higher than for spruce (E_L=10 GPa, σ_t=80 MPa, σ_c=40 MPa, according to DIN 68364 2003) and also compared to hardwoods such as sycamore maple (σ_t=112 MPa, Sonderegger et al. 2012) or European beech (σ_t=97 MPa, Ozyhar et al. 2012b). However, the compression strength in 20ºC/65 % (σ_c=43 MPa) is lower than the reference specie sycamore maple (σ_t=61 MPa, Sonderegger et al. 2012) and European beech (σ_c=45 MPa, Ozyhar et al. 2012b). This leads to a higher tension-compression ratio of σ_t/σ_c=3.0 MPa for ash at standard climatic conditions in the longitudinal direction compared to the species sycamore maple (σ_t/σ_c=1.8, Sonderegger et al. 2012) and European beech (σ_t/σ_c=2.1 MPa, Ozyhar et al. 2012b). The different ratio is due to the much larger decrease of compression strength at increasing EMC compared to the tensile strength.
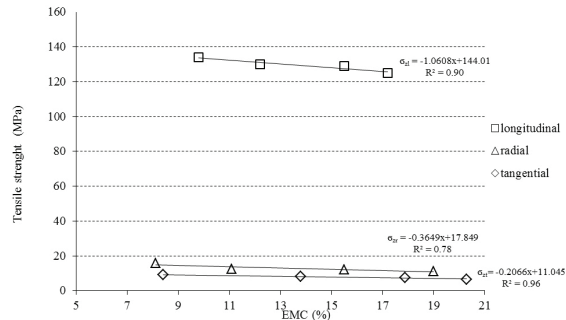

Fig. 2: Tensile strength of common ash in relation to EMC in the main directions.

Fracture toughness

The fracture toughness of ash is higher compared to conifers like spruce or yew. However the values of the current investigation are lower than those obtained by Reiterer et al. (2002). Due to the reinforcing effect of wood rays for a load application in the radial direction, the values of fracture toughness are higher than for TL and TR configurations (Tab. 7). Within a crack plane the fracture toughness was higher if the crack propagated parallel to the grain instead of perpendicular to the grain. In comparison to values for a longitudinal crack propagation direction in sycamore maple, results obtained for ash are 20 % lower, but similar for the RT and TR configurations. The values obtained for European beech by Ozyhar et al. (2012a) are unexpectedly low in comparison. The K_{IC} is highly influenced by EMC in all tested directions, whereas the fracture toughness decreases with increasing EMC.

Tab. 7: Results of the fracture toughness of ash. (n=10); ρ_{12}=0.59–0.63 $g \cdot cm^{-3}$; (ω) = coefficient of variation in %.

TL		TL		RL		RL		TR		TR		RT		RT	
ω (%)		K_{IC} (MPa·m$^{0.5}$)		ω (%)		K_{IC} (MPa·m$^{0.5}$)		ω (%)		K_{IC} (MPa·m$^{0.5}$)		Ω (%)		K_{IC} (MPa·m$^{0.5}$)	
9.9	(4.6)	0.56	(10.5)	9.3	(4.9)	0.78	(6.5)	9.6	(1.2)	0.62	(13.9)	10.2	(1.0)	0.97	(17.6)
13.7	(1.2)	0.49	(7.3)	12.2	(10.9)	0.77	(9.7)	13.8	(0.6)	0.55	(9.7)	14.4	(0.5)	0.85	(12.2)
17.3	(1.4)	0.37	(10.3)	14.9	(0.7)	0.69	(4.8)	17.0	(1.0)	0.49	(14.1)	18.2	(0.7)	0.65	(14.5)
19.2	(1.7)	0.40	(6.2)	18.4	(4.6)	0.65	(10.7)	18.7	(0.6)	0.48	(8.4)	20.1	(0.7)	0.63	(9.1)

CONCLUSIONS

The mechanical, hygric and thermodynamic material properties of ash (*Fraxinus excelsior* L.) were obtained in the moisture range from about 8 to 22 % EMC for the three main anatomical directions. An increase of the EMC causes a decrease in the elastic properties and strength of wood, whereas an increase of the density causes an increase of these properties. Within the hygroscopic range, the investigated values of MOE, shear modulus, strength and fracture toughness decrease linearly to greater or lesser extents. This is consistent with former investigations, however the current results are based on the same material source (a single stem) and therefore build a closed dataset for this species. Similar to the results found for beech by Ozyhar et al. (2012a), the influence of the EMC on the Poisson's ratio of ash is not visible, since the strain in the two directions perpendicular to each other are equally influenced.

A widely closed dataset is provided for the modeling purposes of ash. The dataset enables improved calculations and simulations of multi-layered and three-dimensional wood structures with finite element methods, however rheological properties and the mechano-sorptive behavior was not considered in this work. For a complex material characterization, further research is needed to analyze the plastic behavior, which is particularly important for compression perpendicular to the fiber.

ACKNOWLEDGMENTS

REFERENCES

1. Blumer, S., Niemz, P., Serrano, E., Gustafsson, P.J., 2009: Moisture induced stresses and deformations in parquet floors: An experimental and numerical study. Wood Research 54(1): 89-101.
2. Bodig, J., Jayne, B., 1993: Mechanics of wood and wood composites. 2nd edn., Krieger Publishing, Malabar, Florida, 736 pp.
3. Bonoli, C., Niemz, P., Mannes, D., 2005: Untersuchungen zu ausgewählten Eigenschaften von Eschenholz. Schweiz. Z. Forstwesen. 156(11): 432-437.
4. Bucur, V., 2006: Acoustics of wood. 2nd edn, Springer-Verlag, Berlin, Heidelberg, Germany.
5. DIN 52184, 1979: Testing of wood - determination of swelling and shrinkage.
6. DIN 52185, 1976: Testing of wood - compression test parallel to grain.
7. DIN 52186, 1978: Testing of wood - Bending test.
8. DIN 52187, 1979: Testing of wood - determination of ultimate shearing stress parallel to grain.
9. DIN 52189, 1981: Testing of wood - determination of impact bending strength.
10. DIN 52192, 1979: Testing of wood - compression test perpendicular to grain.
11. DIN 68364, 2003: Properties of wood species - Density, modulus of elasticity and strength.
12. DIN EN ISO 12572, 2001: Hygrothermal performance of building materials and products - Determination of water vapour transmission properties.
13. DIN EN ISO 12737, 2011: Metallic materials - Determination of plane-strain fracture toughness.

14. DIN EN ISO 15148, 2003: Hygrothermal performance of building materials and products - Determination of water absorption coefficient by partial immersion.

15. Gereke, T., Gustafsson, P.J., Persson, K., Niemz, P., 2009: Experimental and numerical determination of the hygroscopic warping of cross-laminated solid wood panels. Holzforschung 63(3): 340-347.

16. Görlacher, R., 1984: Ein neues Messverfahren zur Bestimmung des Elastizitätsmoduls von Holz. Holz als Roh - und Werkstoff 42(6): 219-222.

17. Grosser, D., Teetz, W., 1985: Einheimische Nutzhölzer: Esche. Lose Blattsammlung, Arbeitsgemeinschaft Holz eV, Bonn, Informationsdienst Holz, Centrale Marketinggesellschaft der deutschen Agrarwirtschaft, Bonn, und Arbeitsgemeinschaft Holz e.V., Dusseldorf.

18. Hering, S., 2011: Charakterisierung und Modellierung der Materialeigenschaften von Rotbuchenholz zur Simulation von Holzverklebungen. PhD thesis, ETH Zurich.

19. Horvath, N., Niemz, P., Molnar, S., 2008: Examinations to the influence of wood moisture on chosen wood properties of spruce, oak and beech. Holztechnologie 49(3):10-15.

20. Hering, S., Keunecke, D., Niemz, P., 2012: Moisture-dependent orthotropic elasticity of beech wood. Wood Sci. Technol. 46(5): 927-938.

21. Keunecke, D., 2008: Elasto-mechanical characterization of yew wood and spruce wood with regard to structure-property relationships. PhD thesis, ETH Zurich.

22. Keunecke, D., Sonderegger, W., Pereteanu, K., Lüthi, T., Niemz, P., 2007: Determination of Young's and shear moduli of common yew and Norway spruce by means of ultrasonic waves. Wood Sci. Technol. 41(4): 309-327.

23. Keunecke, D., Hering, S., Niemz, P., 2008: Three-dimensional elastic behaviour of common yew and Norway spruce. Wood Sci. Technol. 42(8): 633-647.

24. Kollmann, F., 1941: Die Esche und ihr Holz. Schriftenreihe Eigenschaften und Verwertung der deutschen Naturhölzer, Band 1., Springer-Verlag, Berlin.

25. Kollmann, F., 1951: Technologie des Holzes und der Holzwerkstoffe. 2nd edn., vol 1. Springer-Verlag, Berlin, 1050 pp.

26. Krackler, V., Keunecke, D., Niemz, P., 2010: Verarbeitung und Verwendungsmöglichkeiten von Laubholz und Laubholzresten. ETH Zurich, 151 pp.

27. Krackler, V., Camatias, U., Ammann, S., 2011: Untersuchungen zum Feuchteverhalten und zur Porosität von thermisch modifiziertem Holz. Bauphysik 33(66): 374-381.

28. Niemz, P., 1993: Physik des Holzes und der Holzwerkstoffe. DRW-Verlag, Leinfelden-Echterdingen, 243 pp.

29. Ozyhar, T., Hering, S., Niemz, P., 2012a: Moisture dependent elastic and strength properties of European beech wood in tension. J. Mater. Sci. 47(16): 6141-6150.

30. Ozyhar, T., Hering, S., Niemz, P., 2012b: Moisture dependent orthotropic tension-compression asymmetry of wood. Holzforschung 67(4): 395-404.

31. Požgaj, A., Chovanec, D., Kurjatko, S., Babiak, M., 1997: Structure and properties of wood. (Štruktúra a vlastnosti dreva). 2nd edn. Priroda, Bratislava, 485 pp (in Slovak).

32. Reiterer, A., Sinn, G., Stanzl-Tschegg, S.E., 2002: Fracture characteristics of different wood species under mode I loading perpendicular to the grain. Mater. Sci. Eng. A. 332: 29-36.

33. Ross, R.J., 2010: Wood handbook. Forest Products Society, Madison WI.

34. Sonderegger, W., Häring, D., Joščák, M., Krackler, V., Niemz, P., 2012: Untersuchungen zur Wasseraufnahme von Vollholz und Holzwerkstoffen. Bauphysik 34(3): 101-106.

35. Szalai, J., 1994: Anisotropic strength and elasticity of wood and wood based composites. University of West Hungary, Sopron.
36. Szalai, J., Niemz, P., Andor, K., Bariska, M., Howald, M., 2004: Untersuchungen zum Einfluss der Holzfeuchtigkeit auf das Bruchverhalten von Fichte bei Zugbelastung in Faserrichtung. Schweiz. Z. Forstwes. 155(1): 1-5.
37. Wagenführ, R., 2007: Holzatlas. 6th edn. Fachbuchverlag, Leipzig, 816 pp.

PETER NIEMZ, SEBASTIAN CLAUSS, FRANCO MICHEL
INSTITUTE FOR BUILDING MATERIALS
ETH ZURICH
STEFANO-FRANSCINI-PLATZ 3
8093 ZURICH
SWITZERLAND
Corresponding author: niemzp@ethz.ch

DANIEL HÄNSCH, ANDREAS HÄNSEL
UNIVERSITY OF COOPERATIVE EDUCATION
HANS-GRUNDIG-STRASSE 25
01307 DRESDEN
GERMANY